

Recoil distance lifetime measurements in ^{69}As and $^{72}\text{Se}^\dagger$

H. P. Hellmeister, E. Schmidt, M. Uhrmacher,* and R. Rascher
Institut für Kernphysik der Universität zu Köln, 5000 Köln 41, Germany

K. P. Lieb
Institut für Kernphysik der Universität zu Köln, Köln, Germany[†]
and Brookhaven National Laboratory, Upton, New York

D. Pantelica
Institute for Atomic Physics, Bucharest, Romania
 (Received 21 November 1977)

High spin state in ^{69}As and ^{72}Se have been excited in oxygen induced reactions on ^{56}Mn , $^{54,56}\text{Fe}$, and ^{58}Ni targets. On the basis of $\gamma\gamma$ coincidences, angular distributions, and excitation functions, a level scheme of ^{69}As is proposed. The following mean lives (in the parentheses) have been determined by the recoil distance Doppler shift method: in ^{72}Se with level energies in keV, 862 (5.2 ± 0.5 ps); 1634 (2.7 ± 0.3 ps); 2466 (2.2 ± 0.3 ps); 3770 (9 ± 3 ps); in ^{69}As , 1307 (1.95 ± 0.05 ns); 2161 (5.1 ± 0.8 ps); 5198 (11.3 ± 1.5 ps). It is suggested that the positive parity states in ^{69}As form a rotational aligned $g_{9/2}$ proton band with $\gamma \simeq 30^\circ$. The presumed $25/2^+$ intruder state features the same deformation as deduced from the $13/2^+ \rightarrow 9/2^+$ $B(E2)$ value.

[NUCLEAR REACTIONS $^{54}\text{Fe}(^{18}\text{O}, p2n)^{69}\text{As}$, $^{56}\text{Fe}(^{16}\text{O}, p2n)^{69}\text{As}$, $^{55}\text{Mn}(^{16}\text{O}, 2n)^{69}\text{As}$, $^{58}\text{Ni}(^{16}\text{O}, \alpha p)^{69}\text{As}$, $^{58}\text{Ni}(^{16}\text{O}, 2p)^{72}\text{Se}$; measured E_γ , relative excitation function, angular distributions, recoil distance Doppler shift; deduced E_x , I^π , $T_{1/2}$, mixing ratio.]

I. INTRODUCTION

The transitional nuclei around $A = 70$ have been found to feature many facts of elementary nuclear excitations. In the even-even nuclei, vibrational and rotational level sequences and the coexistence of both have been encountered.¹⁻³ In many odd- A nuclei, decoupled positive-parity $g_{9/2}$ bands⁴⁻⁶ as well as K mixed negative-parity bands^{7,8} have been identified. The strong influence of the Coriolis force as a consequence of the moderate deformation of $\beta \approx 0.25$ has been first pointed out by Malik and Scholz.⁹ Due to the softness of these nuclei, energy relations between the core and core-plus-particle systems are often seriously disturbed by the extra nucleon. Additional information is required in order to establish the most adequate model description for the odd- A nuclei. Evidently, electric quadrupole matrix elements are appropriate to test collective aspects of these nuclei that are related to their quadrupole deformations.

Information of the nucleus ^{69}As is still rather scarce. Only recently, the ground state spin of $I = \frac{5}{2}$ has been determined in an atomic beam nuclear magnetic resonance NMR experiment.¹⁰ From the β decay of ^{69}Se the Chalk River Group¹¹ established ten states in ^{69}As up to an excitation energy of 2.35 MeV. Nolte *et al.*¹² investigated some presumed high spin states in the reaction

$^{40}\text{Ca}(^{32}\text{S}, 3p)$ whereas Ivanov *et al.*¹³ reported on preliminary recoil distance measurements in which they employed the reaction $^{58}\text{Ni}(^{14}\text{N}, 2pn)$. This latter experiment concentrated on a cascade of several (stretched $E2$?) transitions built on top of the 1306 keV level that Peker,¹⁴ in analogy to similar bands in ^{71}As and ^{73}As (Refs. 5 and 7), interpreted as transitions within a rotational aligned $g_{9/2}$ proton band. It should be noted, however, that the two level schemes proposed in Refs. 12 and 13 are not consistent and that more accurate lifetime measurements are required in order to verify the rotational alignment model in ^{69}As . Due to the complexity of these heavy-ion induced γ -ray spectra, a cross bombardment of the reactions $^{54}\text{Fe}(^{18}\text{O}, 2pn)^{69}\text{As}$, $^{55}\text{Mn}(^{16}\text{O}, 2n)^{69}\text{As}$, $^{56}\text{Fe}(^{16}\text{O}, p2n)^{69}\text{As}$, and $^{58}\text{Ni}(^{16}\text{O}, \alpha p)^{69}\text{As}$ was made, and transition energies, intensities, angular distributions, excitation functions, and lifetimes have been measured.

The level scheme of ^{72}Se has been studied extensively by means of in-beam γ -ray spectroscopy in the reactions $^{70}\text{Ge}(\alpha, 2n)$ and $^{58}\text{Ni}(^{16}\text{O}, 2p)$, and high spin states up to the probable 14^+ member of the ground state band have been identified. Doppler shifted attenuation lifetime measurements for the higher yrast states with $I \geq 8$ have been reported by Hamilton *et al.*,³ Lieb and Kolata,¹⁵ and Lemberg *et al.*¹⁶ As to the lifetimes of the lower yrast states with $I \leq 6$, many results

of Doppler shifted attenuation (DSA) and recoil distance (RD) measurements reported in the literature are in disagreement with each other^{3, 16, 17}. The discrepancies seem to originate from mechanical problems of the plunger apparatus at small distances and/or different assumptions on the feeding mechanism from other discrete levels and the continuum. However, as a “shape transition” from an anharmonic vibration to a rotational band appears to occur around the 4^+ yrast state, the $E2$ decay probabilities of the *low-spin* levels are most interesting from the point of view of nuclear structure, and a remeasurement of them was highly desirable.

II. HIGH SPIN STATES IN ^{69}As

We have studied the γ decays of high spin states in ^{69}As populated in the reactions $^{54}\text{Fe}(^{18}\text{O}, p2n)$, $^{55}\text{Mn}(^{16}\text{O}, 2n)$, $^{56}\text{Fe}(^{16}\text{O}, p2n)$, and $^{58}\text{Ni}(^{16}\text{O}, \alpha p)$. Standard techniques of in-beam γ -ray spectroscopy have been employed including the measurement of $\gamma\gamma$ coincidence spectra, angular distributions, and excitation functions. Table I gives a survey on the type of measurement carried out as well as the target composition and thickness and the beam energy used in each run. Angular distributions and one set of coincidence data have been measured at the MP6 tandem facility of the Brookhaven National Laboratory, simultaneously with an investigation of the reaction $^{58}\text{Ni}(^{16}\text{O}, 2p)^{72}\text{Se}$.¹⁵ Two recoil distance experiments to be discussed in Sec. III have been carried out by means of the FN tandem accelerator of the Institute for Atomic Physics at Bucharest. All other experiments have been performed at the FN tandem laboratory of the University of Cologne.

A. γ -ray energies and yields

Most transitions in ^{69}As have been established from $\gamma\gamma$ coincidence data obtained in the reaction $^{58}\text{Ni}(^{16}\text{O}, \alpha p)$ at 47 and 52.5 MeV beam energy.

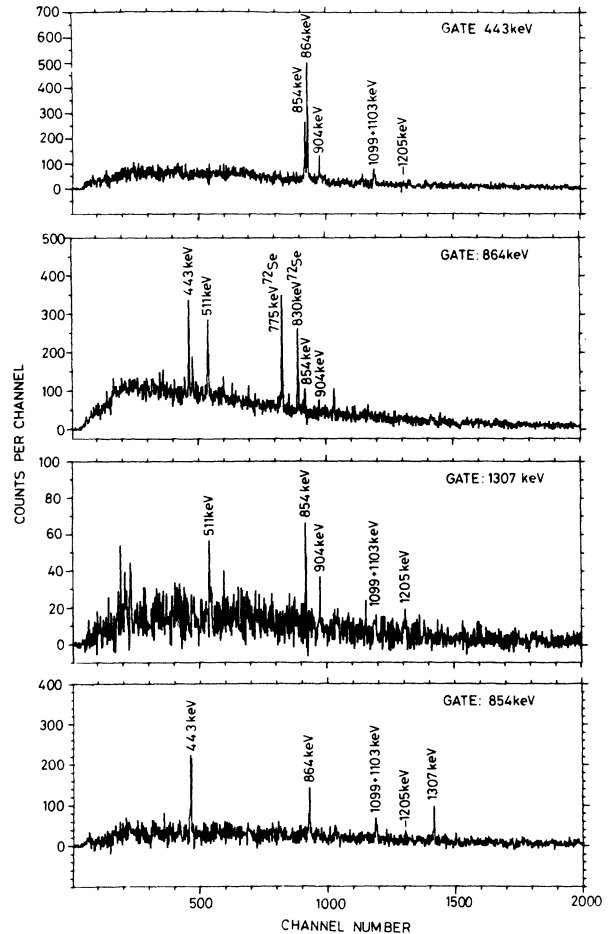


FIG. 1. Some $\gamma\gamma$ coincidence spectra taken in the reaction $^{58}\text{Ni}(^{16}\text{O}, \alpha p)^{69}\text{As}$ at 47 MeV beam energy.

Two Ge(Li) detectors of 10–15% efficiency and energy resolutions of 2.1 to 2.4 keV at 1.33 MeV were placed at angles of $\pm 90^\circ$ (at 47 MeV) and $0^\circ/90^\circ$ (at 52.5 MeV) to the beam. The time resolution of the coincidence setup was typically 20 ns. Coincidence spectra were recorded in event-

TABLE I. Survey on measurements in ^{69}As .

Reaction	E_{lab} (MeV)	Target ($\mu\text{g}/\text{cm}^2$)	Type of measurement	Facility
$^{54}\text{Fe}(^{18}\text{O}, p2n)$	45, 50, 55	210	Energy calibration Excitation function	Köln
$^{55}\text{Mn}(^{16}\text{O}, 2n)$	46	350	$\gamma\gamma$ coincidences	Köln
$^{56}\text{Fe}(^{16}\text{O}, p2n)$	59	300	Recoil distance	Bucharest
$^{58}\text{Ni}(^{16}\text{O}, \alpha p)$	52.5	400	Angular distributions $\gamma\gamma$ coincidences	BNL
	58	280	Recoil distance	Köln
	47	300	$\gamma\gamma$ coincidences	Köln

TABLE II. Energies, angular distribution coefficients, and intensities of transitions in ^{69}As . D indicates a doublet.

Transition E_γ^a (keV)	$E_i, I_i^{\pi i}$	$E_f, I_f^{\pi f}$	Angular distribution ^b			Intensity ^d		
			$100A_2$	$100A_4$	$100\alpha_2$	a	b	c
1306.68(13)	$1307, \frac{9}{2}^+$	$0, \frac{5}{2}^-$	35(4)	0(4)	74(6)	57(3)	59(1)	54(7)
442.70(11)	$1307, \frac{9}{2}^+$	$864, (\frac{7}{2})^-$	-23(3)	0(3)	69(8)	43(2)	41(1)	46(5)
863.98(16)D	$864, (\frac{7}{2})^-$	$0, \frac{5}{2}^-$	D	79(3)	D	60(1)
854.36(12)	$2161, (\frac{13}{2}^+)$	$1307, \frac{9}{2}^+$	27(3)	-9(3)	61(7)	63(3)	73(1)	61(9)
904.1(5)D	$2211, (\frac{11}{2}^+)$	$1307, \frac{9}{2}^+$	-90(6)			<20D	<7	13(4)
1098.7(2)	$3260, (\frac{17}{2}^+)$	$2161, (\frac{13}{2}^+)$	21(5)	5(6)	52(13)	31(3)	50(4)	32(6)
1103.1(5)	$3264, (\frac{15}{2}^+)$	$2161, (\frac{13}{2}^+)$				<22	<13	9(3)
1205.3(2)	$4465, (\frac{21}{2}^+)$	$3260, (\frac{17}{2}^+)$	59(12)	-14(12)	D	27(2)	D	22(4)
733.4(2)D	$5198, (\frac{25}{2}^+)$	$4465, (\frac{21}{2}^+)$	32(6)	-7(8)	80(15)	33(2)D	25(1)	24(6)

^a Measured in the reaction $^{54}\text{Fe}(^{18}\text{O}, p2n)$ at 50 MeV beam energy.

^b Measured in the reaction $^{58}\text{Ni}(^{16}\text{O}, \alpha p)$ at 52.5 MeV beam energy.

^c Measured in the reaction $^{40}\text{Ca}(^{32}\text{S}, 3p)$ at 100 MeV beam energy (Ref. 12).

^d Normalized to the sum of the intensities of the 1307 and 443 keV transitions and corrected for angular distribution.

by-event mode¹⁸ in a matrix of 2028×2048 channels and stored on magnetic tape. Based on the spectra presented in Fig. 1, the lines at 443, 733, 854, 864, 904, 1099, 1103, 1205, and 1307 keV were attributed to transitions in ^{69}As . Unfortunately, the 1103, 733, and 1205, keV transitions which Nolte *et al.*¹² had tentatively placed on top of the 2.16 MeV level, were too weak to allow us to identify their positions in the level scheme. Furthermore, the 863 and 1205 keV lines in the singles spectra are not resolved from strong transitions in ^{72}Se produced in the reaction

$^{58}\text{Ni}(^{16}\text{O}, 2p)$, whereas the 904 and 1099 keV lines overlap with (weak) transitions in ^{71}As formed in the reaction $^{58}\text{Ni}(^{16}\text{O}, 3p)$.⁷ We therefore studied singles spectra of the reaction $^{54}\text{Fe}(^{18}\text{O}, p2n)$ at 45, 50, and 55 MeV beam energy. The two detectors were placed at 0° and 90° to the beam in order to discern any Doppler broadening of the lines. From the 90° spectra, the transition energies given in Table II have been deduced; ^{56}Co and ^{226}Ra sources were used for efficiency and energy calibration.¹⁹ At these bombarding energies, we also determined relative γ ray yields. The excitation functions displayed in Fig. 2 have been corrected for the efficiency of the detectors and the anisotropies of the angular distributions and have been normalized to the sum of the intensities of the 1307 and 443 keV transitions. The 854, 1099, and 1205 keV lines feature the pattern of a high spin cascade. The small intensity variation of the 733 keV transition and its broadened line shape at 0° and 90° reveal that it is a doublet. On the basis of the coincidence data where the 733 keV line is weaker than the 1205 keV line, we placed the former on top of the 1205 keV transition thereby reversing the level ordering proposed previously.^{12, 13}

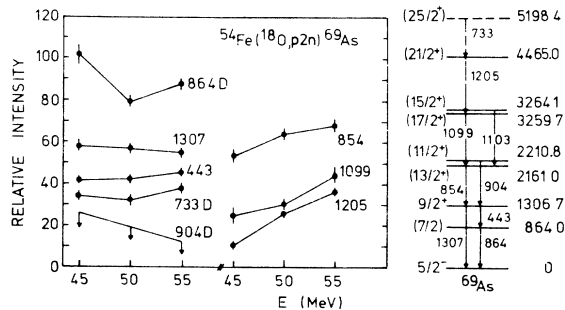


FIG. 2. Excitation functions of transitions in ^{69}As obtained in the reaction $^{54}\text{Fe}(^{18}\text{O}, p2n)$. The intensities have been corrected for the angular distributions and detector efficiency and normalized to the sum of the intensities of the 443 and 1307 keV lines. For the 904 keV line, only an upper limit has been obtained. On the right hand side, the proposed level scheme of high spin states in ^{69}As is given.

In Table II the relative yields of transitions in ^{69}As found in the oxygen induced reactions are compared with that obtained in the reaction $^{40}\text{Ca}(^{32}\text{S}, 3p)$ at 100 MeV beam energy.¹² Good agreement between the $^{54}\text{Fe} + ^{18}\text{O}$ and $^{40}\text{Ca} + ^{32}\text{S}$ systems is found. This is to be expected from the fact that in both systems the average angular

momenta in the compound nuclei are very similar and that the final nucleus is formed after the evaporation of three nucleons. A rough estimate of the grazing angular momentum l_{gr} gives²⁰ $l_{gr}(Fe+O) = 16.3 \hbar$, at 50 MeV beam energy, and $l_{gr}(Ca+S) = 14.2 \hbar$ at 100 MeV.

B. γ -ray angular distributions

The tentative spin assignments indicated in Fig. 2 and Table II are based on the angular distributions obtained in the reaction $^{58}Ni(^{16}O, \alpha p)$ at 52.5 MeV oxygen energy. Spectra were taken between 15° and 165° in 10° intervals and normalized to the intensity of the strong 774 keV $4^+ \rightarrow 2^+$ transition in ^{72}Se produced in the reaction $^{58}Ni(^{16}O, 2p)$ and recorded at 90° in a monitor detector. Angular distribution coefficients A_2 and A_4 are given in Table II. The angular distribution coefficients of the 1307, 854, 1099, and 733 keV transitions are typical for stretched quadrupole transitions, whereas those of the 443 and 904 keV lines exhibit a dipole and mixed dipole/quadrupole character. If we assume that the 733-1205-1099-854-1307 keV cascade is formed by stretched quadrupole transitions (as further corroborated by the measured lifetimes, see below), we arrive at alignment parameters²¹ of $0.52 \leq \alpha_2 \leq 0.80$.

III. RECOIL DISTANCE LIFETIME MEASUREMENTS

A. Experimental procedure and analysis

Previous measurements have indicated^{3, 13, 15-17} that the lifetimes of the levels considered here are in the range between 1 and 10 psec corresponding to flight distances of $D < 50 \mu m$ at a recoil velocity of $v/c = 1.5\%$. Good alignment of the plunger device and very accurate distance monitoring down to zero distance are thus mandatory. The plunger apparatus used has been described previously.²² The flight distance extends between the fixed target and the movable 20 μm thick Ta foil which serves as stopper for the evaporation residues.

Targets were prepared in the following way: Gold foils of 1.0–1.5 μm thickness and 8 cm by 8 cm in size were evaporated onto glass slides and floated off in water. After visual inspection under a microscope, a foil was glued to the cone-shaped target frame and stretched in the plunger device. After this stress test, a target of about 300 $\mu g/cm^2$ was evaporated onto the foil which, except for a central target spot of 10 mm in diameter, was shielded from heat. The target was then stretched again and usually could stand without deterioration a 48 h run with a 50–100 nA oxygen beam. The Ta stopper was mounted in a

similar way. The mechanical accuracy of the distance setting was 1 μm for $D < 800 \mu m$. By checking electrical contact for zero distance and monitoring the capacity at small distances ($D < 200 \mu m$) we have been able to determine lifetimes of less than 1 ps with our plunger device.⁴

In most runs, two Ge(Li) detectors were placed at angles between 0° and 55° . In this way, small contaminants interfering with the Doppler shifted (flight) peaks could be detected. By evaluating the intensity of the Doppler shifted and unshifted peaks and normalizing both to the intensity of a radiation emitted after Coulomb excitation of the Au foil or the Ta stopper, two independent lifetime measurements were done simultaneously for each state. A second reason for considering the Doppler shifted peak was the fact that, in the case of a short lived state populated by a long lived feeder state, the shifted component reveals much more clearly the short lifetime.²³ In order to account for possible feeding from β decay or isomeric states, spectra with good statistics were also taken at large recoil distances up to 7 mm.

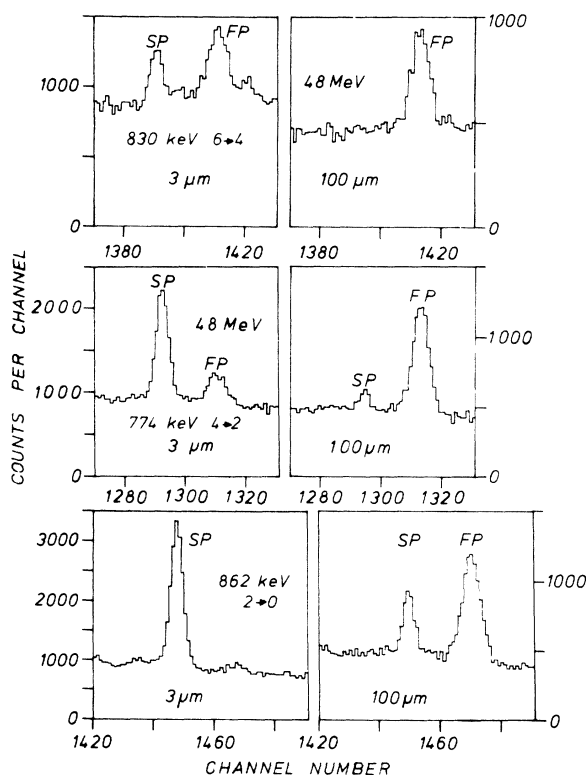


FIG. 3. Portions of the γ -ray spectra taken in the reaction $^{58}Ni(^{16}O, 2p)^{72}Se$ at 48 MeV beam energy. The lines correspond to the unshifted (SP) and Doppler shifted (FP) components of the $6^+ \rightarrow 4^+$, $4^+ \rightarrow 2^+$, and $2^+ \rightarrow 0^+$ transitions.

TABLE III. Experimental parameters for recoil distance Doppler shift measurements.

Run number	Reaction	E_{lab} (MeV)	Recoil velocity ($\mu\text{m}/\text{ps}$)	Position of Ge(Li) detectors (deg)
1	$^{58}\text{Ni}(^{16}\text{O}, 2p)^{72}\text{Se}$	56	5.25(11)	0
2	$^{58}\text{Ni}(^{16}\text{O}, 2p)^{72}\text{Se}$	48	4.80(10)	30, -30
3	$^{58}\text{Ni}(^{16}\text{O}, 2p)^{72}\text{Se}$	58	5.40(11)	0, 50
4	$^{58}\text{Ni}(^{16}\text{O}, 2p)^{72}\text{Se}$	46	4.95(10)	0, 55
3	$^{58}\text{Ni}(^{16}\text{O}, \alpha p)^{69}\text{As}$	58	5.40(11)	0, 50
5	$^{56}\text{Fe}(^{16}\text{O}, p2n)^{69}\text{As}$	59	5.13(12)	0

Figure 3 displays parts of spectra associated with the decays of the 862, 1636, and 2466 keV states in ^{72}Se . Note the clear separation between the respective unshifted (SP) and Doppler shifted (FP) components.

The analysis of the decay functions of the unshifted and Doppler shifted peaks followed the method described in Ref. 22. As discussed for heavy-ion RD experiments in the mass 40 region, the finite spread of the recoil angle and velocity introduces a minor correction. The effect of hyperfine deorientation was neglected for reasons discussed by Rascher *et al.*²⁴ Only in the case of the 862 keV $2^+ \rightarrow 0$ keV transition ($A_2 = 0.14 \pm 0.02$, $A_4 = -0.04 \pm 0.02$ ¹⁵), this effect is much smaller than the 12% error quoted on this lifetime. We also note that for none of the (mostly stretched quadrupole) transitions, an angular dependence of the lifetime has been observed (see Table V).

The major obstacle of RD experiments with heavy-ion fusion reactions is the time delays associated with “continuum” γ rays and the simultaneous population of many discrete feeder states.

The continuum feeding time τ_F has been estimated¹⁵ from DSA analyses of the 7.04 \rightarrow 5.71 MeV $14^+ \rightarrow 12^+$ and 5.71 \rightarrow 4.50 MeV $12^+ \rightarrow 10^+$ yrast transitions in ^{72}Se , at 47–58 MeV beam energy. The experimental upper limit of $\tau_F \leq 0.1$ ps is, fortunately, by more than an order of magnitude shorter than the lifetimes discussed here; continuum feeding has therefore been neglected in the analysis. More serious is the time delay introduced by the finite lifetimes of discrete feeder states, especially when studying low spin states. It is this feeding which has led to discrepancies of up to a factor of three among previous RD measurements in ^{72}Se .^{3, 16, 17} This problem was solved in the following way: In each run we measured the relative intensities P_i and (effective) lifetimes $\bar{\tau}_i$ of the feeder states and incorporated these data in the analysis. Usually, one side feeder and the next one or two yrast feeders were considered.²⁵ In addition, we performed runs at different bombarding energies between 46 and 59 MeV (see Table II) changing in this way the relative contributions of direct (undelayed), yrast, and side feeding. Two sets of feeding parameters in ^{72}Se at 46 and 58 MeV beam energy are given in Table IV and illustrate the higher yrast feeding at 58 MeV. In all cases, the effective yrast feeding

TABLE IV. Relative intensities P and time constants τ of the yrast and side feeding components for states in ^{72}Se .

State (keV)	Run number	E_{lab} (MeV)	Yrast feeding		Side feeding		Direct feeding
			P_{yf} (%)	τ_{yf} (ps)	P_{sf} (%)	τ_{sf} (ps)	P_D (%)
862	4	46	49	2.4	9	12.5(26)	42
	3	58	68	2.5	8		24
1636	4	46	43	2.2	3		54
	3	58	70	2.2	9		21
2466	4	46	8	0.9	20	9(3)	72
	3	58	25	1.2	14		61

TABLE V. Summary on recoil distance measurements in ^{72}Se .

State (keV)	Run	Angle of detector	Mean life τ (ps)		Final value present work	Previous work
			Unshifted peak	Doppler shifted peak		
862	2	-30	5.0(5)	6.0(3)	5.2(5)	3.6(6) ^a
	2	+30	5.5(3)	5.9(3)		5.7(12) ^b
	3	0	4.0(5)	5.4(6)		5.1(6) ^c
	4	0	5.5(5)			
	4	55	3.9(10)	5.9(35)		
1636	1	0	2.1(4)		2.7(3)	1.2(3) ^a
	2	-30	2.8(3)	3.0(3)		4.5 ^{+1.5} _{-1.0} ^b
	2	+30	2.9(8)	3.4(8)		4.5(4) ^c
	3	0	2.1(5)	2.9(4)		
	4	0	2.7(4)	2.5(11)		
	4	55	1.9(5)			
2466	2	-30	2.9(3)	2.1(9)	2.2(3)	<0.7 ^a
	2	+30	2.7(3)	1.7(9)		2.6(7) ^b
	3	0	2.0(3)	2.1(3)		2.0(5)
	4	0	1.8(4)			
3770	3	0	9(3)		9(3)	...

^aReference 17.^bReference 16.^cReference 3.

time $\bar{\tau}_{\text{yf}}$ was close to the “true” lifetime of the next yrast state which decreases continuously for increasing yrast spin.^{15,17}

B. Results in ^{72}Se

For the lowest yrast states in ^{72}Se at 862, 1636, and 2466 keV, up to 10 individual lifetime values have been obtained which are summarized in Table V. Some of the fits to the $R(D)$ decay functions are shown in Figs. 4 and 5. The final numbers have an rms error of 10–15%; they are compared in Table V with the results of previous RD measurements. Our results for the 862 and 2466 keV states are in excellent agreement with those of the Vanderbilt and Leningrad groups, but at variance with Ref. 17. As to the 1636 keV state, we can reproduce the 4.5 ps lifetime reported in Refs. 3 and 16 only when neglecting delayed feeding totally in the analysis of the stopped component. We also note that Lemberg *et al.*¹⁶ assumed a feeding time of $\tau_{\text{yf}} = 0.9 \pm 0.3$ ps in their analysis. When inserting the longer lifetime $\tau(2466) = 2.2 \pm 0.3$ ps of the most important feeder state, they would obtain $\tau(1636) \approx 3.5$ ps, in better agreement with our result. As to the interpretation of the results, the reader may refer to our previous paper on the structure of the ^{72}Se ground state band.¹⁵

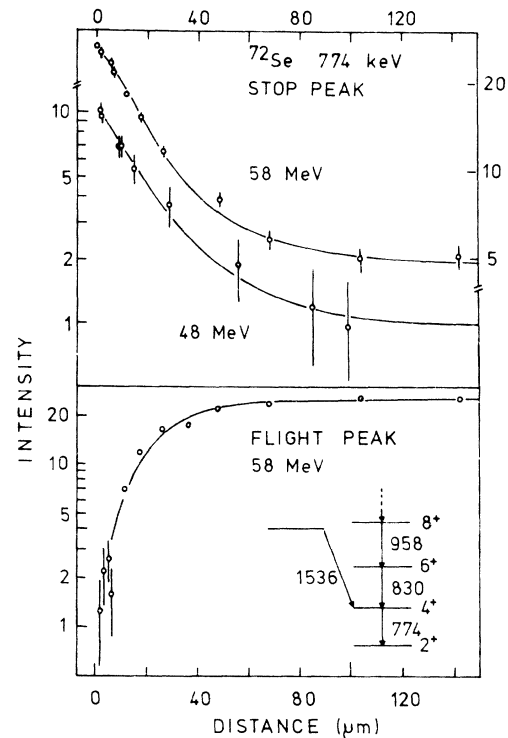


FIG. 4. Recoil distance plots of the stopped and shifted components of the 774 keV $4^+ \rightarrow 2^+$ transition in ^{72}Se . The insert indicates the feeder states considered in the analysis.

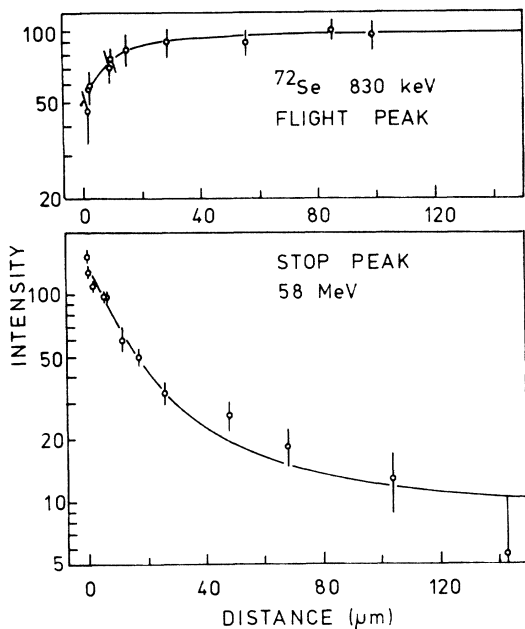


FIG. 5. Same as Fig. 4, but for the 830 keV $6^+ \rightarrow 4^+$ transition in ^{72}Se .

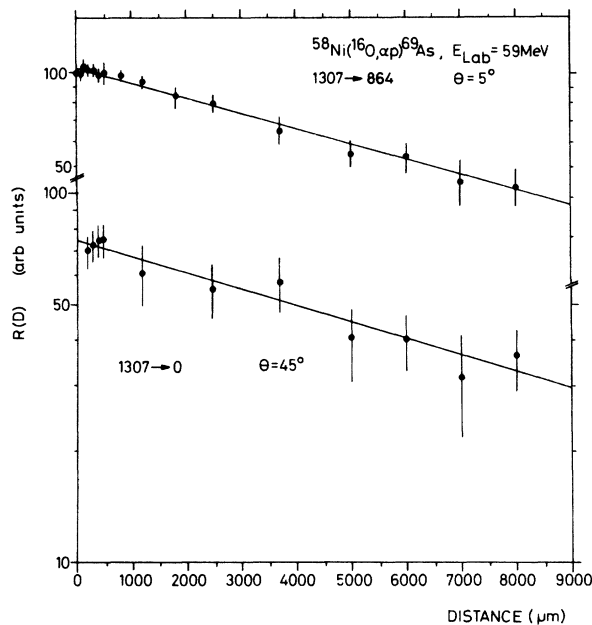


FIG. 6. Recoil distance plot for the decay of the 1307 keV $\frac{3}{2}^+$ state in ^{69}As .

C. Results in ^{69}As

From the $R(D)$ decay functions of transitions in ^{69}As , some of which are presented in Figs. 6 and 7, we deduced the lifetimes given in Table VI. Most of them are in good agreement with the preliminary, less precise data of the Leningrad group.¹³ For the 3260 and 4465 keV states, only upper limits are given since the amount of side and cascade feeding could not be determined well enough due to the doublet nature of the 1205 keV line. A small Doppler broadening of this transition observed at 0° in the reaction $^{54}\text{Fe}(^{19}\text{O}, p2n)$ where this line is not perturbed, allows us to place a lower limit of $\tau(4465) > 0.5$ ps. The observation of this broadening, on the other hand, puts some doubt on the value $\tau(4465) = 9.5 \pm 2.0$ ps reported in Ref. 13. One should finally keep in mind that very similar effective time constants are found for the unshifted components of the 1205 and 733 keV transitions, both in Ref. 13 and the present work. As the 4465 keV state is predominantly fed via the 733 keV transition, a short lifetime of this state would be masked by the long lifetime of the 5198 keV level. The Doppler shifted component of the 1205 keV transition on the other hand overlaps with the 1205 keV shifted component associated with the decay of the short lived 5.07 MeV state in ^{72}Se ¹⁵ and was thus not analyzed.

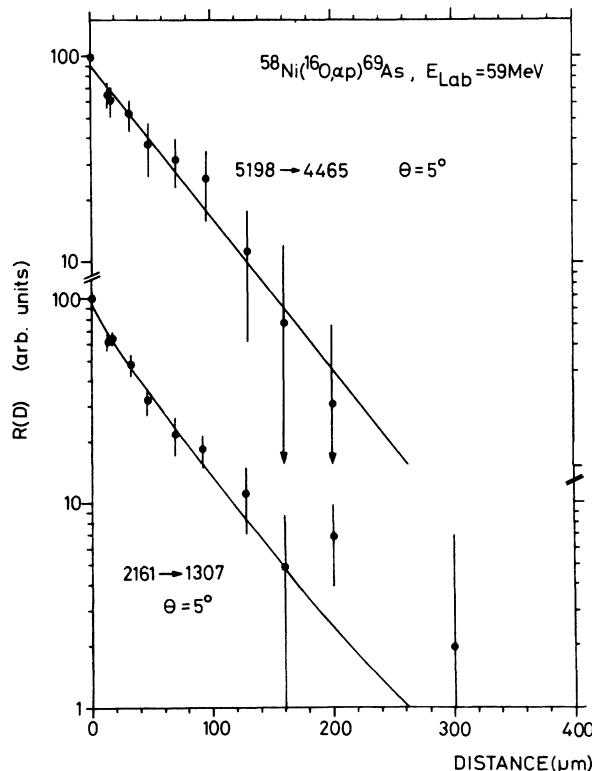


FIG. 7. Same as Fig. 6., but for the 854 and 733 keV transition in ^{69}As .

TABLE VI. Summary of recoil distance measurements in ^{69}As .

State	Transition E_γ (keV)	Run	Angle	Present work	Mean life τ (ps)	
					Reference 13	Adopted value
1307	443	3	0	1910(60)	1900(200)	1940(50)
		3	50	1920(50)		
	1307	3	0	1910(100)		
		3	50	2110(100)		
		5	0	<u>2090(420)</u>		
				1950(60)		
2161	854	3	0	4.9(12)	6(3)	5.2(8)
		3	50	<u>5.3(12)</u>		
				5.1(8)		
3260	1099	3	0	<8	<6	<6
		5	0	<13		
4465	1205	3	0	7.1(13) ^a	9.5(20)	<12
		3	50	6.8(27) ^a		
		5	0	11(4) ^a		
5198	733	3	0	10.7(14)	8(2)	9.6(16)
		3	50	<u>11.8(17)</u>		
				11.3(15)		

^a Assuming $\tau_{\text{st}} = 11.3(15)$ ps and $P_{\text{st}}/P_D = 2.0(5)$.

IV. DISCUSSIONS AND CONCLUSIONS

A. Level structure of ^{69}As

The 1307 keV state. This state decays by the 443 and 1307 keV γ rays with branching ratios of $(42 \pm 1) : (58 \pm 1)\%$. The long lifetime of 1.95 ± 0.05 ns and the quadrupole type angular distribution of the 1307 keV transition favor an assignment of $I^\pi(1307) = \frac{9}{2}^+$. If we adopt the alignment coefficient $\alpha_2(1307) = 0.74 \pm 0.06$ in the analysis of the 443 keV angular distribution and assume $I(864) = \frac{7}{2}$, we arrive at a mixing ratio of $\delta(443) = 0.01 \pm 0.04$, indicating a pure dipole nature of this transition.

The 2161 keV state. This state has a mean life of $\tau = 5.2 \pm 0.8$ ps and decays by a quadrupole type transition. Both findings make a spin-parity assignment of $I^\pi(2161) = \frac{13}{2}^+$ very probable.

The 2211 keV state. This state decays to the 2161 keV level as proved by the coincidence data. The small intensity of the 904 keV line indicates that it is not a member of the yrast cascade. Similar nonfavored states have been observed in the heavy ion reactions leading to $^{71,73}\text{As}^\tau$ and $^{69,71}\text{Ge}^{26}$ as shown in Fig. 8. The short lifetime of $\tau < 2$ ps¹³ and the large quadrupole/dipole mixing ratio of $\delta(904) = -1.0 \pm 0.5$ derived from the angular distribution are compatible with the tentative assignment of $I^\pi = \frac{11}{2}^+$.

The 3260 and 4465 keV states. These states form a cascade of stretched quadrupole transitions populating the 2161 keV $\frac{13}{2}^+$ state. Their short lifetimes of $\tau(3260) < 6$ ps and $0.5 < \tau(4465) < 12$ ps rule out $M2$ character and favor spin-parity assignments of $\frac{17}{2}^+$ and $\frac{21}{2}^+$, respectively.

The 3264 keV state. This state is based on rather weak arguments. Its decay to the 2161 keV level follows from the coincidence spectra, but the 1103 keV line is not well enough separated from the (stronger) 1099 keV line in order to establish its exact intensity. From the $0^\circ/90^\circ$ intensity ratio obtained in the reaction $^{54}\text{Fe}(^{18}\text{O}, p2n)$, a negative A_2 coefficient is found which, together with the short lifetime of $\tau < 2$ ps¹³ and the analogy to neighboring nuclei (see Fig. 10) makes the assignment $I^\pi = \frac{15}{2}^+$ not implausible.

The 5198 keV level. This level, finally, has a lifetime of $\tau = 9.6 \pm 1.6$ ps and decays by a 733 keV radiation to the 4465 keV state. Again, the angular distribution is typical for a stretched quadrupole transition which then leads to our tentative assignment of $I^\pi = \frac{25}{2}^+$ for this level.

B. Comparison of positive-parity high spin states in the Ge and As isotopes

Turning to Fig. 8, we shall now compare in some detail the energies of $E2$ decay probabilities

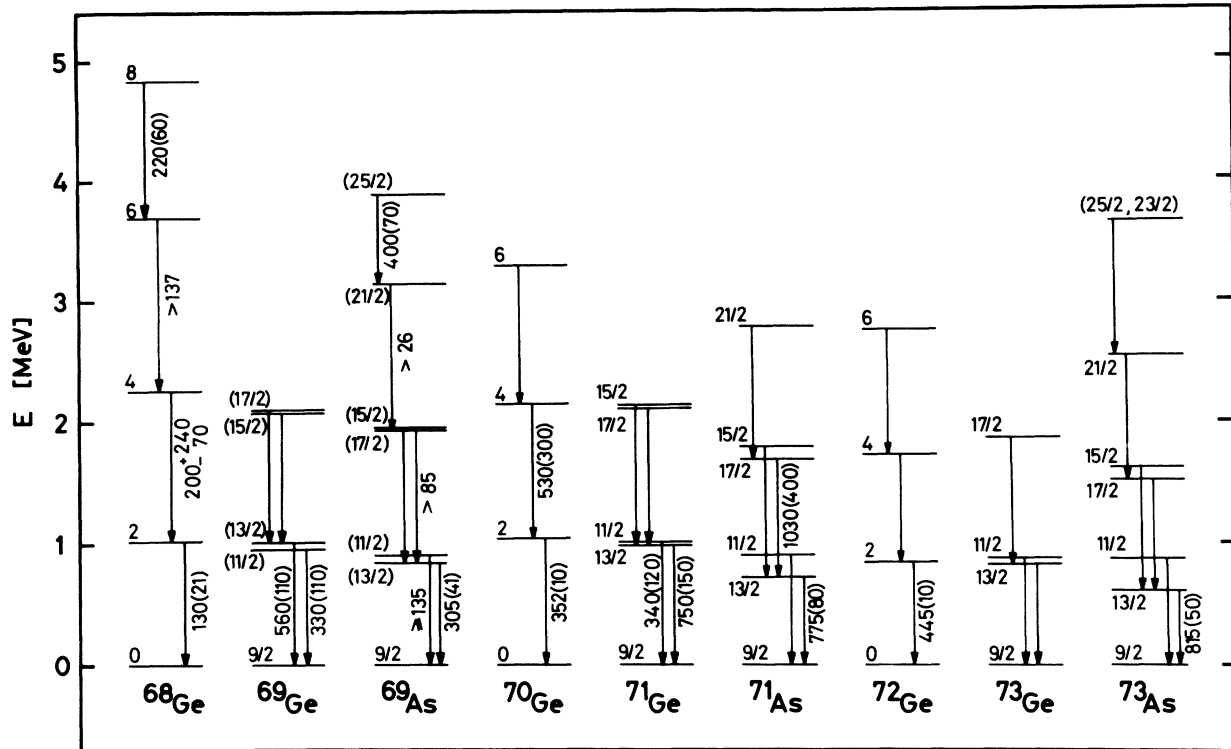


FIG. 8. Comparison of positive-parity high spin states in odd As and Ge isotopes with the core spectra of the even Ge isotopes. $B(E2)$ values are given in $e^2 \text{fm}^4$.

of these high spin states in ^{69}As with the neighboring odd Ge and As isotopes^{5, 7, 26} as well with the even Ge core configurations. The spectra of the odd nuclei have been shifted as to bring the respective $\frac{9}{2}^+$ states to zero excitation energy; all $B(E2)$ values are given in units of $e^2 \text{fm}^4$.

In terms of a simple core-plus-particle picture for the odd nuclei some general trends are evident:

- (1) There is rather good agreement in energy between the even Ge core spectra and the odd Ge states. The energy splittings between the lowest $\frac{13}{2}$ and $\frac{11}{2}$ states and between the $\frac{17}{2}$ and $\frac{15}{2}$ states are surprisingly small being only 27 keV on the average to be compared with a core energy of about 1 MeV.
- (2) The As spectra, on the other hand, are considerably lower than the Ge core states and much closer to the respective states of the even Se isotopes⁷. The $\frac{13}{2} - \frac{11}{2}$ splitting increases from 50 keV in ^{69}As to 256 keV in ^{73}As , whereas the $\frac{17}{2} - \frac{15}{2}$ splitting is of the order of 4–100 keV.
- (3) Both ^{68}Ge and ^{69}As show a pronounced “back-bending” effect at $I^\pi = 8^+$ and $I^\pi = \frac{25}{2}^+$, respectively.
- (4) Going from ^{68}Ge to ^{72}Ge , the $B(E2, 2^+ \rightarrow 0^+)$ value increases from $130 \pm 21 e^2 \text{fm}^4$ to $445 \pm 10 e^2 \text{fm}^4$. The $E2$ strengths of the $\frac{13}{2}^+ \rightarrow \frac{9}{2}^+$ transitions

also increase slightly, but they are in all cases a factor of 1.7 to 4.3 larger than the core transition probabilities. This fact rules out a simple weak-coupling interpretation.

Several models have been proposed to understand these properties of the odd nuclei and to relate them to those of the core states. We mention the rotational alignment coupling (RAC) scheme²⁷ with symmetric^{5, 7} or triaxial²⁸ shape of the core as well as the particle vibrational coupling (PVC) scheme^{29, 30} with one or three valence nucleons. It was soon realized that the most simple RAC approach²⁷ in which a $g_{9/2}$ particle is coupled to a symmetric rigid rotor does not work very well in this mass region.⁵ This model predicts $B(E2, \frac{13}{2}^+ \rightarrow \frac{9}{2}^+) / B(E2, 2^+ \rightarrow 0^+) = 1.4$ whereas one finds that this ratio exceeds 1.7 in all cases (2.3 ± 0.5 in ^{69}As). The drop in energy of the $\frac{13}{2}^+$ states in $^{71, 73}\text{As}$ and the larger $B(E2)$ values have been interpreted by Heits *et al.*^{5, 7} as due to further polarization of the core due to the extra particle. A further deficiency of the model is that the unfavored $\frac{11}{2}^+$ and $\frac{15}{2}^+$ states are much too high⁷ and, even more important, that the energies of the Ge core states deviate considerably from a rotational band.

A better parametrization of the core taking into

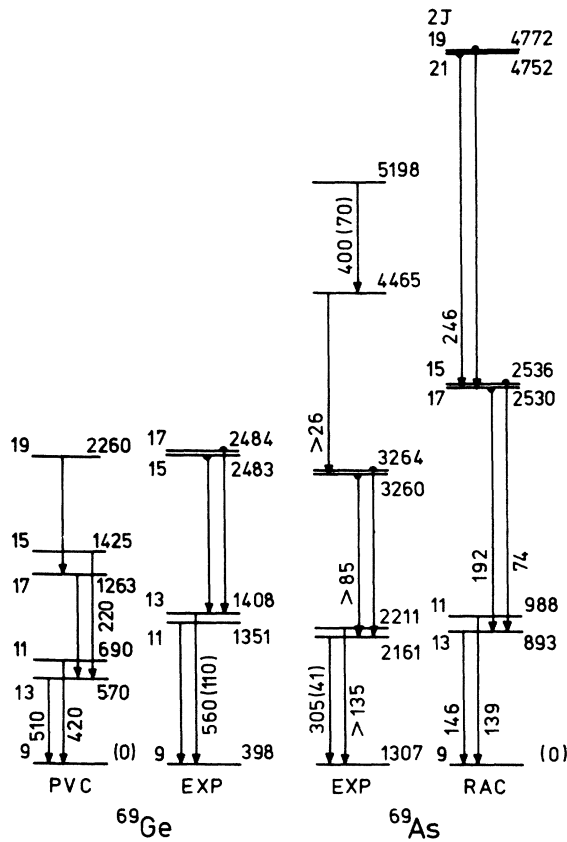


FIG. 9. Comparison of positive-parity high spin states in ^{69}As and ^{69}Ge with the prediction of the RAC and PVC models (Ref.30).

account γ deformation and variable moment of inertia (VMI) has been proposed by Toki and Faessler.²³ For the positive-parity states in ^{73}As , they obtained fair agreement with the parameters $\hbar^2/2\theta = 139$ keV, $\beta = 0.25$, and $\gamma = 26.6^\circ$ taken from the ^{72}Ge core. In this approach, the small energy splittings between the $\frac{13}{2}^+$ and $\frac{11}{2}^+$ state and between the $\frac{17}{2}^+$ and $\frac{15}{2}^+$ state are closely related to the triaxiality of the core.³¹ For $\gamma = 30^\circ$, this level crossing occurs around $\beta = 0.2$ (see Fig. 5b of Ref. 31). In spite of the success of the model, it underestimates the $B(E2)$ value of the $\frac{13}{2}^+ \rightarrow \frac{9}{2}^+$ transition and overestimates the energy of the $\frac{13}{2}^+$ state by about 20% suggesting again a further polarization of the core.

We have applied this model to ^{69}As making use of recent results on its core nucleus ^{68}Ge .³² A very sensitive measure of the γ deformation is the strength of the ground state transition from the 2_1^+ state. The experimental ratio of $B(E2, 2_2 \rightarrow 0_1)/B(E2, 2_1 \rightarrow 0_1) = 0.025 \pm 0.006$ (Ref. 32) gives $\gamma = 26.6 \pm 0.5^\circ$, identical to the value obtained in ^{72}Ge . A fit to the energies of the 1017 keV 2_1 ,

1779 keV 2_2 , and 2268 keV 4_1 core states gives $\hbar^2/2\theta = 153$ keV, whereas $\beta = 0.14$ is taken from $B(E2, 2_1 \rightarrow 0_1)$. Placing the Fermi energy at $\lambda = -3.87$ MeV and using a pairing energy constant of $\Delta = 1.44$ MeV,²⁸ one obtains the RAC spectrum displayed in Fig. 9. The relative splittings of the yrast and nonfavoured states are well reproduced, but the higher band members are too high in energy indicating the need of VMI.²⁸ One may argue that the assumption of *rigid* triaxial shapes with γ fixed conflicts with the softness of the even Ge isotopes. Yamazaki³³ has indeed pointed out that the energies and $E2$ transition probabilities of the ground state and γ band are rather insensitive to the softness of the nucleus. The same argument holds for the Coriolis coupled spectrum of the odd nucleus as recently demonstrated by Dönau and Frauendorf³⁴ for the case of the $i_{13/2}$ band in ^{191}Pt where $\beta = 0.20$ and $\gamma \approx 30^\circ$ were found.

Paar *et al.*³⁰ described the positive-parity states in $^{69,71}\text{Ge}$ in terms of the particle-vibrator coupling scheme by coupling a cluster of three $\{g_{9/2}, d_{5/2}\}$ quasiparticles to phonon states. The phonon energy $\hbar\omega = 0.83$ MeV and effective charge $e_{\text{vib}} = 3e$ were fixed from the energy and $E2$ decay probability of the 2_1 state in ^{72}Ge . This core was chosen since the negative-parity states in ^{69}Ge were interpreted as $\{p_{3/2}, f_{5/2}, p_{1/2}\}$ three hole clusters. Using a particle vibration coupling constant of $a = 0.4$, these authors obtain $B(E2, \frac{13}{2}^+ \rightarrow \frac{9}{2}^+) = 510 e^2 \text{fm}^4$ in agreement with the experimental figures.²⁶ Due to the low phonon energy, the spectrum is somewhat compressed (see Fig. 9). Furthermore, the very small energy splitting between the yrast states and the respective nonfavoured $\frac{11}{2}^+$ and $\frac{15}{2}^+$ states are not too well reproduced; these states would be degenerate in the case of *one* $g_{9/2}$ particle.³⁰ The point to be stressed is the fact that the ^{72}Ge core used in the calculation of the particles states in ^{69}Ge already accounts to a large extent for the polarization which the odd particle exerts on the less collective ^{68}Ge core.

Recently, de Lima *et al.*³² found evidence for three closely lying 8^+ states in ^{68}Ge to which they assigned different internal structures. The 4838 keV 8^+ (yrast) state and the 5050 keV 8^+ state are suggested to be the bandheads of $\nu(g_{9/2}^2)$ and $\pi(g_{9/2}^2)$ bands, whereas the energy of the 5367 keV 8^+ state fits well into the pattern of the ground state band. By the same reasoning, Peker¹⁴ proposed that the 5198 keV ($\frac{25}{2}^+$) state in ^{69}As arises from the coupling of a $g_{9/2}$ proton to the $\nu(g_{9/2}^2)8^+$ neutron state. We already mentioned that the γ -ray energies from both "intruder" states are considerably smaller than the normal in-band transitions. It might therefore be interesting to know what effect this change of internal structure has on

the $B(E2)$ values. We first note that the measured ratio $B(E2, 8 \rightarrow 6)/B(E2, 2 \rightarrow 0) = 1.7 \pm 0.5$ in $^{68}\text{Ge}^{32}$ agrees with the prediction of the asymmetric rotor model for $\gamma = 27^\circ$ where this ratio is 1.94 (Ref. 28). Furthermore, the experimental ratio $B(E2, \frac{25}{2} \rightarrow \frac{21}{2})/B(E2, \frac{13}{2} \rightarrow \frac{9}{2}) = 1.3 \pm 0.3$ of transitions in ^{69}As is in good agreement with the Coriolis coupling scheme^{27,28} which predicts this ratio to be 1.4. We therefore conclude that the $E2$ decay strengths of both "intruder" states do *not* indicate any appreciable change of deformation within either ^{68}Ge or ^{69}As . This finding is difficult to understand in view of the drastic change in deformation when going from ^{68}Ge to ^{69}As .

C. Effective coupling constants for $1g_{9/2} \rightarrow 1f_{5/2}$ $M2$ transitions

The present measurement on the lifetime of the 1307 keV $\frac{9}{2}^+$ state also adds information on the $M2$ coupling constants of $1g_{9/2} \rightarrow 1f_{5/2}$ single quasiparticle transitions. Similar $\frac{9}{2}^+ \rightarrow \frac{5}{2}^-$ transitions have been identified in other Zn, Ge, As isotopes, in ^{81}Br and in ^{85}Rb (Refs. 35 and 36). The respective $B(M2)$ values and effective coupling constants $g^{\text{eff}}/g^{\text{s.p.}}$ (relative to the single-particle limit $g^{\text{s.p.}} = g_s - \frac{2}{3}g_1$) are summarized in Table VII, where g^{eff} is defined by the relation³⁷

$$B(M2, \frac{9}{2}^+ \rightarrow \frac{5}{2}^-) = \frac{3}{5\pi} \mu_0^2 \langle r \rangle^2 (g^{\text{eff}})^2 (\frac{5}{2} \frac{1}{2} 2 0 | \frac{9}{2} \frac{1}{2})^2, \quad (1)$$

where μ_0 denotes the nuclear magneton. The radial matrix element has been approximated by $\langle r \rangle = 0.75 r_0 A^{1/3}$ with $r_0 = 1.2$ fm.

In Fig. 10, we have plotted $g^{\text{eff}}/g^{\text{s.p.}}$ versus the

TABLE VII. $M2$ transition strengths between the $1g_{9/2}$ and $1f_{5/2}$ single-particle orbits.

Nucleus	E_γ (keV)	$B(M2)$ ($\mu_0^2 \text{fm}^2$)	$g^{\text{eff}}/g^{\text{s.p.}}$ ^a	$g^{\text{eff}}/g^{\text{sqp}}$ ^b
^{67}Zn	604	2.72(11)	0.175(3)	0.17(2)
^{67}Ge	734	2.39(24)	0.164(8)	0.25(3)
^{69}Ge	398	2.62(9)	0.170(3)	0.18(2)
^{71}Ge ^b	24.0	1.49(7)	0.127(5)	0.21(5)
^{69}As ^c	1307	5.7(2)	0.197(5)	
^{71}As	1001	2.55(5)	0.129(1)	0.21(2)
^{73}As	361	1.47(8)	0.097(3)	0.18(2)
^{75}As	24.5	1.45(7)	0.096(3)	0.26(5)
^{77}As	211	1.02	0.080	0.22
^{81}Br	274	0.89(2)	0.073(1)	0.17(2)
^{85}Rb	514	1.47(2)	0.093(1)	0.18(2)

^a $g^{\text{s.p.}}$ calculated according to Eq. (1).

^b Reference 36; g^{sqp} calculated according to Eq. (2).

^c Present work.

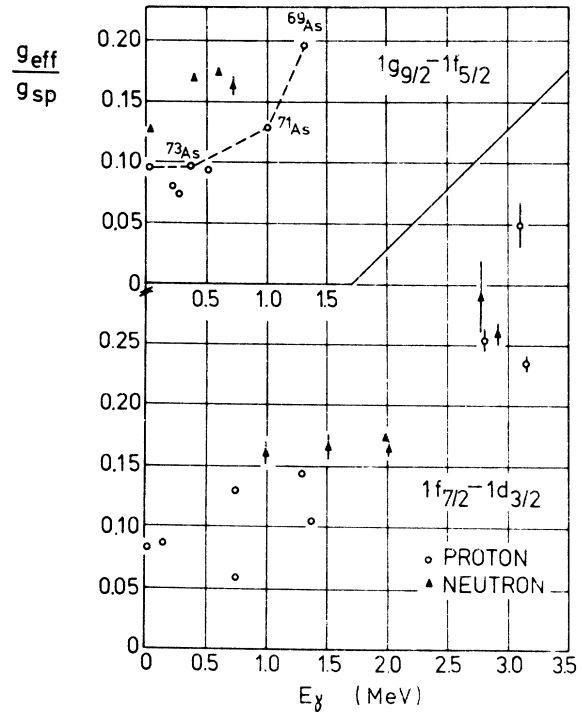


FIG. 10. Summary of effective $M2$ coupling constants $g^{\text{eff}}/g^{\text{s.p.}}$ of single-particle transition in $A < 90$ nuclei.

transition energy E_γ . It may be first noted that g^{eff} is in all cases much smaller than the single-particle estimate. This retardation which also occurs for the $1f_{7/2} \rightarrow 1d_{3/2}$ and $1h_{11/2} \rightarrow 2f_{7/2}$ quasi-single-particle transitions, has been traced by Ejiri *et al.*³⁸ to the destructive effect of the spin-isospin core polarization. Superimposed on this general inhibition is a trend which we recently also observed in the $A = 40$ region, namely a correlation between g^{eff} and E_γ .³⁹ A similar correlation also persists for the $1g_{9/2} \rightarrow 1f_{5/2}$ $M2$ transitions in the odd As isotopes where $g^{\text{eff}}/g^{\text{s.p.}}$ increases from 0.08 (^{77}As) to 0.20 (^{69}As). According to Ejiri,³⁷ one may write

$$g^{\text{eff}} = (U_{9/2}U_{5/2} + V_{9/2}V_{5/2})C_{9/2}C_{5/2} \frac{1}{F} g^{\text{s.p.}} = \frac{1}{F} g^{\text{sqp}}, \quad (2)$$

where the retardation factor $F > 1$ accounts for the effect of the core polarization, $U_{5/2}$, $U_{9/2}$, $V_{5/2}$, and $V_{9/2}$ denote the usual pairing factors of the $1f_{5/2}$ and $1g_{9/2}$ orbits, and $C_{5/2}$ and $C_{9/2}$ the respective single-particle amplitudes. Taking the U , V , and C from the ($^3\text{He}, d$) spectroscopic factors measured by Betts *et al.*,⁴⁰ one finds indeed that $g^{\text{eff}}/g^{\text{sqp}} \approx 0.20$.

V. CONCLUSIONS

The present study on the properties of positive-parity high spin states in ^{69}As has illustrated two aspects of the interplay between the $1g_{9/2}$ single-proton state and collective degrees of freedom of the ^{68}Ge core. The $M2$ matrix element of the $1307\text{ keV } \frac{9}{2}^+ \rightarrow \frac{5}{2}^-$ transition is hindered by a factor of 5 with respect to the single-particle estimate and reflects the effect of the $M2$ giant resonance. Evidence for a Coriolis coupled band built upon the $g_{9/2}$ proton state and extending up to $I^\pi = \frac{25}{2}^+$ is presented. Like in the neighboring odd Ge and As isotopes,^{7,26} this band shows very small energy splittings between the yrast and unfavored states. An interpretation has been given in the frame of the rotational aligned coupling scheme and particle vibrational coupling scheme. Both approaches are about equally successful in predicting the level ordering (if the γ degree of freedom with $\gamma \approx 30^\circ$ is taken into account in the RAC scheme). Both models, however, fail in predicting sufficient $E2$ strength in the $\frac{13}{2}^+ \rightarrow \frac{9}{2}^+$ transition, if the adjacent even Ge isotope is taken as the core. Due to the softness of these cores, the core properties are

only qualitatively retained in the core-plus-particle systems and a further polarization of the core by the extra particle is evident in all cases. Finally, it has been found that the $B(E2)$ value of the presumed $\frac{25}{2}^+ \rightarrow \frac{21}{2}^+$ "backbending" transition in ^{69}As is not associated with an appreciable change of deformation.

ACKNOWLEDGMENT

The authors gratefully acknowledge the help of F. J. Bergmeister, Dr. J. Eberth, Professor J. J. Kolata, and V. Zobel during various stages of the experiment. Discussion with Professor G. Alaga, Professor H. Ejiri, Professor A. Gelberg, Professor J. Meyer-ter-Vehn, Professor P. K. Peker, and Professor P. von Brentano have been essential in understanding the experimental results, and we would like to express our gratitude. The collaboration has been supported by the Deutsches Bundesministerium für Forschung und Technologie, the United States Energy Research and Development Agency, and the Auslandsbüro des Kernforschungszentrums Karlsruhe.

*Present address: CERN, Geneva, Switzerland.

†Supported by BMFT and U. S. E. R. D. A.

‡Permanent address.

¹J. Hadermann and A. C. Rester, Nucl. Phys. **A231**, 120 (1974).

²A. Bohr and B. R. Mottelson, *Nuclear Structure* (Benjamin, New York, 1975), Vol. II.

³J. H. Hamilton *et al.*, Phys. Rev. Lett. **36**, 340 (1976); and references cited therein.

⁴H. G. Friederichs, A. Gelberg, B. Heits, K. P. Lieb, K. O. Zell, M. Uhrmacher, and P. von Brentano, Phys. Rev. Lett. **34**, 745 (1975).

⁵B. Heits, H. G. Friederichs, A. Gelberg, K. P. Lieb, A. Perego, R. Rascher, K. O. Zell, and P. von Brentano, Phys. Lett. **61B**, 33 (1976).

⁶P. von Brentano, B. Heits, and C. Protop, in *Problems of Vibrational Nuclei*, edited by G. Alaga, L. Sips, and V. Paar (North-Holland, Amsterdam, 1975), p. 155.

⁷B. Heits, H. G. Friederichs, A. Rademacher, K. O. Zell, and P. von Brentano, Phys. Rev. C **15**, 1742 (1977).

⁸K. O. Zell, doctoral thesis Univ. of Köln, 1978 (unpublished).

⁹W. Scholz and F. B. Malik, Phys. Rev. **176**, 1355 (1968).

¹⁰H. A. Helms, W. Hogervorst, G. J. Zaal, and J. Blok, Phys. Scr. **14**, 138 (1976).

¹¹H. Schmeing, T. Faestermann, J. C. Hardy, R. L. Graham, J. S. Geiger, H. R. Andrews, and K. P. Jackson, Chalk River Progress Report No. AECL-5315, 1976 (unpublished), p. 17.

¹²E. Nolte, Y. Shida, W. Kutschera, R. Prestele, and H. Morinaga, Z. Phys. **268**, 267 (1974).

¹³M. A. Ivanow, I. Kh. Lemberg, and I. S. Michin, in

Annual Conference on Nuclear Spectroscopy (Soviet Academy of Sciences, Baku, USSR, 1976) p. 410.

¹⁴P. K. Peker, in *Annual Conference on Nuclear Structure*, (Soviet Academy of Sciences, Leningrad, USSR, 1975), p. 206.

¹⁵K. P. Lieb and J. J. Kolata, Phys. Rev. C **15**, 939 (1977).

¹⁶I. Kh. Lemberg, *et al.*, Annual Conference on Nuclear Spectroscopy (see Ref. 14), p. 376.

¹⁷K. E. G. Löbner *et al.*, Z. Phys. **A274**, 251 (1975).

¹⁸H. W. Schuh, program LISTMODE, Univ. of Köln 1975 (unpublished).

¹⁹V. Zobel, J. Eberth, U. Eberth, and E. Eube, Nucl. Instrum. Methods **141**, 329 (1977); V. Zobel, thesis, Univ. of Köln, 1976 (unpublished).

²⁰H. V. Klapdor, H. Reiss, and G. Rosner, Nukleonika **21**, 763 (1976).

²¹T. Yamazaki, Nucl. Data **A3**, 1 (1967).

²²K. P. Lieb, M. Uhrmacher, J. Dauk, and A. M. Kleinfeld, Nucl. Phys. **A223**, 445 (1974).

²³K. P. Lieb and M. Uhrmacher, Z. Phys. **267**, 399 (1974).

²⁴R. Rascher, M. Uhrmacher, and K. P. Lieb, Phys. Rev. C **13**, 1217 (1976); K. P. Lieb, A. M. Nathan, and J. W. Olness, Hyperfine Interactions (to be published).

²⁵H. P. Hellmeister, program CRONOS, Univ. of Köln 1976 (unpublished).

²⁶J. Eberth, J. Eberth, E. Eube, and V. Zobel, Nucl. Phys. **A257**, 285 (1976).

²⁷F. S. Stephens, Rev. Mod. Phys. **47**, 43 (1975).

²⁸H. Toki and A. Faessler, Phys. Lett. **63B**, 121 (1976); Z. Phys. **A276**, 35 (1976).

²⁹G. Alaga, in *Nuclear Structure and Nuclear Reactions*,

- Proceedings of the International School of Physics, "Enrico Fermi," Course XL*, edited by M. Jean and R. A. Ricci (Academic, New York, 1969), p. 28.
- ³⁰V. Paar, U. Eberth, and J. Eberth, *Phys. Rev. C* **13**, 2532 (1976).
- ³¹J. Meyer-ter-Vehn, *Nucl. Phys. A* **249**, 111 (1975).
- ³²G. M. Gusinski, *et al.*, Annual Conference on Nuclear Spectroscopy (see Ref. 14); p. 376; A. F. de Lima *et al.*, *Proceedings of the International Conference on Nuclear Structure, Tokyo, 1977*, (North-Holland, Amsterdam (1977), Contributed papers, p. 276.
- ³³T. Yamazaki, in *Colloque Franco-Japonais, Dogashima* edited by Y. Shida (Institute for Nuclear Study, University of Tokyo, 1976), p. 480.
- ³⁴F. Dönau and S. Fauendorf, Proceedings of the Tenth Mazurian School in Nuclear Physics, 1977 (unpublished).
- ³⁵Nuclear Data Group, *Nuclear Data Sheets 1959-1965* (Academic, New York, 1966).
- ³⁶S. Nakayama, T. Kishimoto, Y. Nagai, T. Itahashi, T. Shibata, and H. Ejiri, *Proceedings of the International Conference on Nuclear Structure* (see Ref. 32), Contributed papers, p. 275.
- ³⁷A. Bohr and B. R. Mottelson, *Nuclear Structure* (Benjamin, New York, 1975), Vol. I, p. 388.
- ³⁸H. Ejiri, *Nucl. Phys. A* **166**, 594 (1971).
- ³⁹J. Keinonen, R. Rascher, M. Uhrmacher, N. Wüst, and K. P. Lieb, *Phys. Rev. C* **14**, 169 (1976).
- ⁴⁰R. R. Betts, S. Mordachai, D. J. Pullen, B. Rosner, and W. Scholz, *Nucl. Phys. A* **230**, 232 (1974).